Permeable Reactive Barriers as Long-Term Solutions for Groundwater Remediation:

Dynamics of Groundwater Properties, Methane Concentrations, Dissolved Inorganic Carbon Concentrations, and Rates of Carbon Oxidation Processes, Across the NITREX Permeable Reactive Barrier in Waquoit Bay, Cape Cod

Kaitlyn S. Lucey

Wellesley College
Wellesley, Massachusetts 02481 USA

Abstract

The purpose of this experiment was to investigate the dynamics of groundwater properties, methane concentrations, dissolved inorganic carbon (DIC) concentrations, and rates of carbon oxidation processes, across a permeable reactive barrier (PRB) to access the microbial metabolism of the barrier as the initial steps in determining the effectiveness of PRBs as long-term agents for groundwater remediation. Data was collected during neap tide conditions and spring tide conditions in order to determine the effects of saltwater intrusion on the dynamics of the barrier.

It was determined from specific conductivity, temperature, pH, and dissolved oxygen profiles, that the barrier functions differently under neap and spring tide conditions. Specific conductivity values in the barrier were greater under spring tide conditions as compared to neap tide conditions. Temperature profiles indicated that the flow path of groundwater changes as a result of saltwater intrusion. Moreover, while patterns in pH were similar during neap and spring tide conditions, pH of the groundwater was generally more basic during spring tides. In addition, the barrier is relatively anaerobic profile during neap tide conditions, yet during spring tide conditions, the system is inundated with aerated water.

Concentrations of methane and DIC in and around the barrier were discovered to be correlated under both neap tide and spring tide conditions. In addition, both methane and DIC concentrations in the PRB were almost twice as large during neap tide conditions than during spring tide conditions. In general, although methane concentrations were seen to be elevated within the barrier, differences in methane concentrations inside and outside the barrier were relatively small. Moreover, concentrations of methane were in general two to three orders of magnitude less than concentrations of DIC. Thus, while methane is correlated with dissolved organic carbon, at the instances the barrier was sampled, methanogenesis was not a major process of carbon oxidation occurring in the PRB. Methanogenesis could very well be a dominant process under different conditions, however, and determining this requires more fine scale analysis of the barrier over a longer period of time.

The rate of methane production (methanogenesis) was determined to be approximately 0.5µmol L-1d-1, nitrogen reduction (maximum potential denitrification) to be approximately 2.5µmol L-1d-1, and carbon oxidation to be approximately 240µmol L-1d-1 during a neap tide. The rate of methane production (methanogenesis) was determined to be approximately 0.3µmol L-1d-1, nitrogen reduction (maximum potential denitrification) to be approximately 10µmol L-1d-1, and carbon oxidation to be approximately 96µmol L-1d-1 during a spring tide. As a result, methanogenesis does not play a significant role in the carbon oxidation occurring in the barrier under the conditions investigated, especially the case during periods of abnormally high saltwater intrusion. Overall, this data indicate that saltwater intrusion greatly impacts the microbial metabolism of the barrier, and that the barrier is extremely dynamic on a short time scale.

Key words:
Permeable Reactive Barriers, groundwater remediation, methane, dissolved inorganic carbon, neap tide, spring tide, carbon oxidation, denitrification, methanogenesis, sulfate reduction

Introduction

Eutrophication in open, coastal waters results in harmful algae blooms, widespread fish kills, and other ecosystem-altering consequences, and can in-part be attributed to nitrogen loading from the groundwater. Sources of groundwater nitrogen, such as wastewater, septic systems, and fertilizer applications, are a product of residential and commercial development, and abound on the developed coasts of Cape Cod. In order to determine a solution to this problem, an experimental, NITREX Permeable Reactive Barrier, was installed at the groundwater/estuarine interface at the head of Waquoit Bay (Fig. 1).

Permeable Reactive Barriers (PRBs) installed across the flow path of contaminated groundwater, use natural groundwater flow conditions for remediation (Manuel 1998). These barriers allow the passage of water while prohibiting the movement of contaminants (Manuel 1998). Agents such as zero-valent metals, sorbents, and microbes within the barrier either degrade or retain the contaminants (Manuel 1998). The goal of such installations is to eliminate the possibility that a contaminated groundwater plume can discharge into surface waters (Manuel 1998). In particular, the reason for the installation at Waquoit Bay is to facilitate denitrification in nitrogen-enriched groundwater before it enters the surface water of the Bay. The NITREX material of the PRB serves a carbon substrate to fuel denitrification, and is effectively woodchips.

Ideally, nitrate (NO_3^-) does not penetrate through the PRB. Reactions occurring up gradient of the barrier, such as denitrification and dissimilatory nitrate reduction to ammonium (DNRA), change NO_3^- into N_2 gas or ammonium (NH_4^+) respectively, before NO_3^- has the chance to enter surface waters. Immobilization, another possible mechanism for occluding the passage of NO_3^- into surface waters, is a process by which the NO_3^- becomes bound to the substrate's surface.

Dissolved inorganic carbon in the form of CO_2, is a product of both the denitrification and DNRA reactions. Preliminary data that has measured dissolved inorganic carbon in microcosms of the barrier indicates that there are sources of dissolved inorganic carbon other than the aforementioned reactions (unpublished data).

Because the production of CO_2 demonstrates how much carbon from the NITREX barrier is being consumed, and because the barrier will stop working when all the carbon is utilized, it is important to assess the processes that are consuming the woodchips as they could impact the life expectancy of the barrier and in turn, its effectiveness as a long term solution to groundwater remediation. Additional sources of carbon oxidation could include sulfate reduction and fermentation reactions.

Denitrification is a more energetically favorable reaction than sulfate reduction. In turn, sulfate reduction is a more energetically favorable reaction than fermentation. While nitrogen is supplied to the barrier through contaminated groundwater, saltwater intrusion supplies sulfate to the barrier. Saltwater intrusion depends on tide and storm activity, and neap tides and spring tides conditions can influence the amount of saltwater reaching the barrier. Neap tides are when the tide's range is at its minimum whereas spring tides are when the tide's range is at its maximum. In our system, at the time data was obtained, the highest neap tide reached around Well 23, whereas the highest spring tide reached around Well 29. In the absence of nitrogen and sulfate, fermentation should become the dominant carbon oxidation reaction in the barrier. Methanogenesis is when fermentation produces methane. Other fermentation products were not measured in this experiment.

As the modern landscape changes and develops rapidly, it has become increasingly important to understand the effects of nutrient loading and to monitor nutrient movement between terrestrial and aquatic ecosystems. As the initial steps in assessing the durability and effectiveness of PRBs as long-term agents for groundwater remediation, methane and dissolved inorganic carbon concentrations were investigated in the groundwater across the barrier to determine if there is a significant amount of methanogenesis occurring in the barrier. Rates of individual carbon oxidation processes occurring in the PRB were quantified. This study is unique in that while PRBs installed in freshwater ecosystems have been monitored, PRBs in a saltwater ecosystem has not yet been assessed. The barrier was examined during a neap tide and a spring tide to determine if saltwater intrusion had an impact on the microbial metabolism in the barrier. In all, groundwater properties and the data above were obtained to investigate the dynamics of the processes occurring in the barrier. Ultimately, this barrier example could provide useful information in regards to a less-expensive alternative to wastewater treatment for Town of Falmouth and other coastal communities.

Methods

Sampling

An experimental PRB, 4m wide, 2m deep, and 20m long, consisting of a carbon substrate to promote denitrification, was installed at the head of Waquoit Bay in 2005 (Fig. 1). Although upon installation lime was added to the PRB, it is assumed that all that lime was gone by the time this experiment took place. Wells were installed at various locations and depths in and around the barrier. Prior to sampling, the pipelines of the wells were purged. Groundwater was sampled on three different days to generate two data sets: November 16, 2006 (Data Set 1), November 21, 2006 (Data Set 1), and December 5, 2006 (Data Set 2). Data Set 1 was obtained under neap tide conditions, whereas Data Set 2 was obtained under spring tide conditions. On November 16, 2006, groundwater was sampled from one well that was installed up-gradient of the barrier (Well 26) at depths of 1.0m, 1.5m, 2.0m, 2.5m, 3.0m, 3.5m, 4.0m, and 4.5m, three wells within the barrier (Wells 27, 28, and 29) at depths of 1.0m, 1.5m, 2.0m, and 2.5m, 1.0m, 1.5m, 2.0m, and 2.5m, and of 1.0m, 1.5m, and 2.0m respectively, and one well that was installed down-gradient of the barrier (Well 23) at depths of 0.6m, 1.0m, 1.7m, and 2.2m. On November 21, 2006, groundwater was sampled from Well 29 at 4.0m, Well 23 at 0.6m and 1.0m, and Well 22 at 0.8m, 2.0m, and 2.4m. On December 5, 2006, groundwater was sampled from Well 26 at depths of 1.0m, 1.5m, 2.0m, 2.5m, 3.0m, 3.5m, 4.0m, and 4.5m, Well 27 at depths of 1.0m, 1.5m, 2.0m, and 3.5m, Well 28 at depth of 1.0m, 1.5m, 2.0m, 2.5m, 3.0m, 3.5m, and 4.0m, Well 29 at depths of 1.0m, 1.5m, 2.0m, 2.5m, 3.0m, and 4.0m, Well 23 at depths of 0.6m, 1.0m, 1.4m, 1.7m, 2.2m, and 2.6m, and Well 22 at depths of 0.4m, 0.8m, 2.0m, and 2.4m.

A Geotech, Geopump Peristaltic Pump (Geotech Environmental Equipment, Inc.: Denver, Colorado) was used to pump groundwater to the surface. A Hydrolab Quanta (Austin, Texas) was used to measure specific conductivity, temperature, pH, and concentrations of dissolved oxygen. Samples were collected in 20mL plastic syringes and syringes were then placed in water and on ice to minimize leakage of gas until they were analyzed for methane and dissolved inorganic carbon (DIC) less than 24 hours after sampling.

Gas Chromatography

Groundwater samples were analyzed for methane and DIC with a Shimadzu Gas Chromatograph GC-14A with a Poropak Q column. Prior to analysis, samples of room air, CO_2 scrubbed air, and standards including 500.00, 1250.00, and 20100.00ppm CO_2 as well as 15.30, 100.00, and 2000.00ppm CH4, were run.

Samples were approximately 1°C-4°C when analyzed. Syringes were emptied until 5mL of sample remained, then 15.00mL of CO_2–scrubbed air was drawn into the syringe for a total air water volume of 20.00mL. Approximately 3µL of 1N H_2SO_4 was added to the sample through a rubber membrane and for approximately 1 minute, the syringe was shaken to equilibrate the methane and CO_2 between the air and water. 15.00mL of air was injected from the syringe into the Gas Chromatograph, and measurements of methane and DIC were taken.

Calculations of Methane and DIC Concentrations

Areas of methane generated from the Gas Chromatograph were multiplied by the attenuation factor the machine was set to at the time the readings were taken. Areas of the samples were converted to units of ppm using the respective linear equations from the standard curves derived from plotting the areas of the standards against their given concentrations. Afterwards, the data in units of ppm was converted to concentrations using the Ideal Gas Law. In this experiment:

$$n = \frac{(PV)}{(RT)} = \frac{\left(\left(\frac{ppm}{10^6}\right)\left(\frac{15}{1000}\right)\right)}{((0.08205)(293))}$$

Calculations of DIC from Respiration

DIC from respiration was calculated from total DIC concentrations, using the standard mixing model below:

$$DIC_C = \left(\left(\frac{(SpC - SpC_{GW})}{(SpC_{WB} - SpC_{GW})}\right)(DIC_{WB} - DIC_{GW})\right) + DIC_{GW}$$

Where SpC is the specific conductivity measured in a well,

SpC_{GW} is the SpC in the groundwater obtained from the lowest value found in

Well 26 in mS/cm (= 0.009 mS/cm),

SpC_{WB} is the SpC in Waquoit Bay in mS/cm (= 50.00mS/cm),

DIC_{GW} is the DIC used for SpC_{GW} in µmol, and

DIC_{WB} is the DIC in Waquoit Bay in µmol (= 2.06µmol).

Calculations of Rates of Reactions

Assuming that the barrier is at steady state with its surroundings, I used the equation below to calculate the rates of the carbon oxidation reactions occurring in the PRB:

$$R = \left(\frac{Q}{V}\right)\left(C^o - C^i\right)$$

Where R is the rate of the reaction in µmol L-1 d-1,

Q is the ground flow rate in m/d (=0.33m/d),

V is the depth of the PRB in m (=2.00m),

C^o is the final concentration in µmol/L, and

C^i is the initial concentration in µmol/L.

Results

Specific Conductivity

During neap tide conditions, specific conductivity across the barrier and its surroundings was in general, the highest in the middle of the barrier and overall the highest in Well 28 at a depth of 1.5m (Fig. 2). During spring tide conditions, specific conductivity was again highest in Well 28 at a depth of 1.5m in addition to Well 28 at a depth of 1m, and Well 29 at depths of 1m, 1.5m, and 2m (Fig. 3). While specific conductivity values were similar in the other locations inside the barrier and surrounding system under both neap and spring tide conditions, ranging from 0.009mS/cm to 13.96mS/cm, specific conductivity in the middle of the barrier were relatively smaller under neap tide conditions than spring tide conditions, ranging from values of 14.80mS/cm to 18.40mS/cm and relatively larger under spring tide conditions than neap tide conditions, ranging from 20.10mS/cm to 28.90mS/cm (Figs. 2 and 3).

Temperature

Temperature profiles indicate the direction of groundwater flow (Figs. 4 and 5). During neap tide conditions, the temperature profile shows a distinct flow of groundwater in the direction of Well 26 to Well 22 (Fig. 4). This pattern is changed, however, during spring tide conditions, and a distinct injection of saltwater is seen to intrude Wells 28, 29, 23, and 22 at the uppermost depths, 1.0m and 1.5m, 1.0m, 0.6m, and 0.4m respectively (Fig. 5). In addition, during neap tide conditions, temperature inside the barrier and surrounding system was greater than during spring tide conditions, ranging from 10.52°C to 12.75°C (Fig. 4). During spring tide conditions, temperature inside the barrier and surrounding system was smaller than during neap tide conditions, ranging from 7.92°C to 10.85°C (Fig. 5).

pH

The pH of groundwater sampled during neap tide conditions and spring tide conditions showed similar trends, increasing in value from Well 26 to Well 22, ranging from a pH of 4.95 to 7.20 across the gradient of the barrier (Figs. 6 and 7). Overall, the pH of the groundwater during neap time conditions is slightly more acidic, however, then the pH of the groundwater during spring tides (Figs. 6 and 7). Specifically, the pH of the barrier ranges from 4.95 to 6.77 during neap tides and 5.21 to 7.20 during spring tides (Figs. 6 and 7).

Dissolved Oxygen

The patterns in dissolved oxygen in groundwater during neap tide conditions showed increasingly anoxic conditions from Well 26 to Well 22 at values of 5.97 mg/L to 0.32 mg/L respectively (Figs. 8 and 9). Under these conditions, the barrier was relatively anoxic. In general, the amount of dissolved oxygen in groundwater was greater during spring tides than neap tides, and ranged from 0.5mg/L to 7.62mg/L (Figs. 8 and 9). Moreover, whereas under neap tide conditions, the plume of oxygenated groundwater did not reach Wells 27 through 22, oxygenated water was seen from Wells 26 to 29 under spring tide conditions and infiltrates the barrier (Figs. 8 and 9). Under spring tide conditions, a band of anoxic water is detected around Wells 29, 23, and 22 (Fig. 9).

Methane and DIC

Concentrations of methane and DIC in and around the barrier were correlated under both neap tide and spring tide conditions (Figs. 10, 11, 12, and 13). This is especially the case under neap tide conditions where concentrations were greatest inside the barrier (Figs. 10 and 12). Concentrations of methane, however, were in general two to three orders of magnitude less than concentrations of DIC (Figs. 10, 11, 12, and 13). Methane concentrations were twice as large during neap tide conditions compared to during spring tide conditions and ranged from 0.26µmol/L to 5.77µmol/L under neap tide conditions and 0.99µmol/L to 2.98µmol/L under spring tide conditions (Figs. 10 and 11). Moreover, DIC concentrations nearly doubled during neap tides than during spring tides and ranged from 11.70µmol/L to 1960.00µmol/L under neap tide conditions and 362.45µmol/L to 1308.17µmol/L under spring tide conditions (Figs. 12 and 13). In addition, under both tide conditions, although methane concentrations were elevated within the barrier, differences in methane concentrations inside and outside the barrier were relatively small (Figs. 10 and 11). Furthermore, on November 21, methane concentrations appear highest at all depths of Wells 23 and 22 (Fig. 10).

Rates of Metabolic Processes Occurring in the Barrier

The rate of methane production (methanogenesis) was determined to be approximately 0.5μmol L-1d-1, nitrogen reduction (maximum potential denitrification) to be approximately 2.5μmol L-1d-1, and carbon oxidation to be approximately 240μmol L-1d-1 during a neap tide. The rate of methane production (methanogenesis) was determined to be approximately 0.3μmol L-1d-1, nitrogen reduction (maximum potential denitrification) to be approximately 10μmol L-1d-1, and carbon oxidation to be approximately 96μmol L-1d-1 during a spring tide.

Discussion

Data indicate that the barrier functions quite differently under neap and spring tide conditions, suggesting that the barrier is greatly impacted by saltwater intrusion as a result of varying tidal activities. Thus, it can be inferred that the carbonate chemistry of barrier is extremely dynamic on a small scale. In experiments where groundwater being intruded by saltwater was monitored, it was also concluded that saltwater intrusion varied greatly with tides, storm activity, seasons, and year to year (Narayan *et al.* 2003). It comes as no surprise then, that a system sensitive to saltwater intrusion, such as the PRB, would be highly dynamic.

Specific conductivity, temperature, pH, and DO measurements taken from the barrier during a neap tide and a spring tide show pronounced disparities between the two conditions, indicating the highly dynamic quality of the barrier. Data showed that saltwater intrusion changes the natural flow pattern of the groundwater. Saltwater intrusion has been traced in groundwater systems close sources of saltwater, and in those investigations, the flow of groundwater closest to the saltwater source, was indeed changed (Tihansky 2005). Likewise, pH values decrease under spring tide conditions showing that saltwater intrusion affects the pH of the barrier. Moreover, DO data show an anaerobic profile of the groundwater under neap tide conditions, yet during a period of saltwater intrusion the system is flushed with oxic water. It is speculated that within a few hours after that data was taken, that the barrier returned to anoxic conditions. This emphasizes how dynamic the barrier is on a small scale. Results from an experiment in which bacteria who rely on DO were used to treat groundwater, show that DO in groundwater is quite variable across space and depth and can be influenced by influxes of saltwater (Smith *et al.* 2005). This data serves to strengthen the portrayal of the barrier as a dynamic system highly influenced by saltwater intrusion.

Data indicate that methane and DIC concentrations are correlated, suggesting that methanogenesis is a process of carbon oxidation occurring in the barrier. Because methane concentrations were significantly lower than DIC concentrations, however, under the conditions at which samples were taken, methanogenesis was not a major process of carbon oxidation occurring in the PRB. In particular, because methane concentrations are half as large under spring tides as opposed to neap tides, methanogenesis does not play a significant role in the carbon oxidation occurring in the barrier, especially under spring tides. Furthermore, that both rates of methane production (methanogenesis) and nitrogen uptake (denitrification) are less than the overall rate of carbon oxidation occurring in the barrier, furthers that methanogenesis does not contribute significantly to the carbon oxidation occurring in the barrier at the time data was taken. In addition, the plume of methane on 21st quite possibly represents the plume of methane on 16th being ejected from the barrier. This emphasizes the dynamics of the barrier. This is not to say that methanogenesis is not a significant player in carbon oxidation in the barrier. For example, methanogenesis could very well be a dominant process during different times of the year, as during this season in particular, spring tides and saltwater intrusion are at their strongest. Investigations into the chemistry and hydrogeology of groundwater show that characteristics of groundwater do in fact vary seasonally (Fraser *et al.* 1998). That the snapshots of the barrier obtained during this project are representative of the barrier at two specific instances during the year, furthers the notion that the carbonate chemistry of the barrier is extremely dynamic.

That methane concentrations are greatly lower than DIC concentrations in and around the barrier, coupled with the fact that methanogenesis and denitrification rates are less than carbon oxidation rates, suggests that sulfate reduction is the most prevalent process of carbon oxidation occurring in the PRB. Because methane concentrations are even lower during spring tides, and that the rates of methanogenesis and denitrification are smaller than the rates of carbon oxidation especially during spring tides, indicates that saltwater intrusion greatly impacts the chemistry of the barrier and favors sulfate reduction as a process of carbon oxidation.

From the data obtained during this experiment, it can be concluded that the PRB is extremely dynamic and is greatly affected by tidal activity. In order to produce a more accurate portrayal of the dynamics of the barrier, the system beckons for more fine scale work over a longer period of time then this experiment investigated the barrier. In fact, most research of microbial-induced remediation oversimplifies the multifarious properties if an aquifer (Christ *et al.* 2005). In order to generate a more precise picture of the dynamics in the barrier, it would be wise in the future to install in situ sensors to take hourly measurements. Similar experiments into factors that affect remediation properties support that it is integral to understand as much detail possible about the remediation system in order to assess its effectiveness (Palmer *et al.* 1991).

Acknowledgments

First and foremost, I would like to thank my advisor, Joe Vallino, for his guidance throughout the duration my project. I would like to thank Ken Foreman as well, for his assistance and support during the initial stages of my project. I am appreciative of Jane Tucker's help using the Gas Chromatograph. I would like to extend my gratitude to Jessica Mark-Welch, Jen Culbertson, Christina Romero, and Linda Zettler and her laboratory assistants Susie and Erika, for their guidance with molecular techniques. Finally, I would like to thank Rich McHorney and the SES TAs, Laura, Clara, and Beth, for their assistance both in the lab and in the field.

Literature Cited

Manuel, J. 1998. Clearer Water: It's Elementary. Environmental Health Perspectives **106**:332-334.

Narayan, K. A., C. Schleeberger, P. B. Charlesworth, and K. L. Bristow. 2003.

Effects of Groundwater Pumping On Saltwater Intrusion In The Lower Burdekin Delta, North Queensland. Modeling and Simulation Society of Australia and New Zealand **2**:224-229.

Tihansky, A. B. 2005. Effects of Quifer Heterogeneity on Ground-Water Flow and Chloride Concentrations in the Upper Floridan Aquifer near and within an Active Pumping Well Field, West-Central Florida. U.S. Geological Survey Scientific investigations Report **5268**:75.

Smith, A. E., K. Hristova, I. Wood, D. M. Mackay, E. Long, and D. Lorenzana. 2005. Comparisson of Biostimulation versus Bioaugmentation with Bacterial Strain PM1 for Treatment of Groundwater Contaminated with Methyl Tertiary Butyl Ether. Environmental Health Perspectives **113**:317-322.

Fraser, B. G., and D. Williams. 1998. Seasonal Boundary Dynamics of a Groundwater/ Surface-Water Ectone. Ecology **79**:2019-2031.

Christ, J. A., A. C. Ramsbury, L. M. Abriola, K. D. Pennell, and F. E. Loffler. 2005. Coupling Aggressive Mass Removal with Microbial Reductive Dechlorination Remediation of DNAPL Source Zones: A Review and Assessment. Environmental Health Perspectives **113**:465-477.

Palmer, C. D., and P. R. Wittbridt. 1991. Processes Affecting the Remediation of Chromium-Contaminated Sites. Environmental Health Perspectives **92**:25-40.

Figures and Tables

Figure 1. Location of NITREX Permeable Reactive Barrier in Waquoit Bay, Cape Cod.

Figure 2. Conductivity in and around the barrier under neap tide conditions on November 16 (black point) and November 21 (black circle around black point).

Figure 3. Conductivity in and around the barrier under spring tide conditions.

Figure 4. Temperature in and around the barrier under neap tide conditions on November 16 (black point) and November 21 (black circle around black point).

Figure 5. Temperature in and around the barrier under spring tide conditions.

Figure 6. pH in and around the barrier under neap tide conditions on November 16 (black point) and November 21 (black circle around black point).

Figure 7. pH in and around the barrier under spring tide conditions.

Figure 8. DO in and around the barrier under neap tide conditions on November 16 (black point) and November 21 (black circle around black point).

Figure 9. DO in and around the barrier under spring tide conditions.

Figure 10. Methane concentrations in and around the barrier under neap tide conditions on November 16 (black point) and November 21 (black circle around black point).

Figure 11. Methane concentrations in and around the barrier under spring tide conditions.

Figure 12. DIC concentrations in and around the barrier under neap tide conditions on November 16 (black point) and November 21 (black circle around black point).

Figure 13. DIC concentrations in and around the barrier under spring tide conditions.

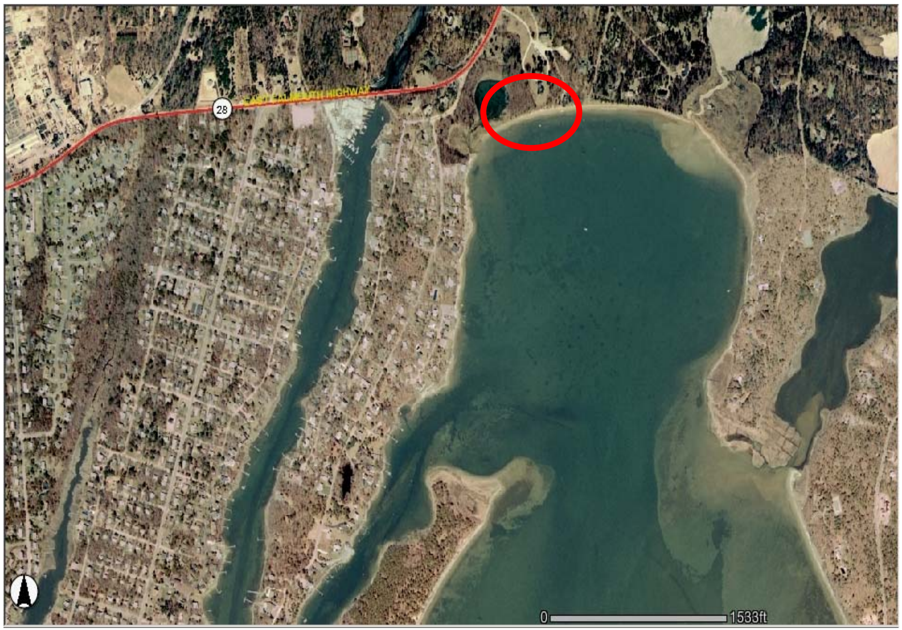

Figure 1.

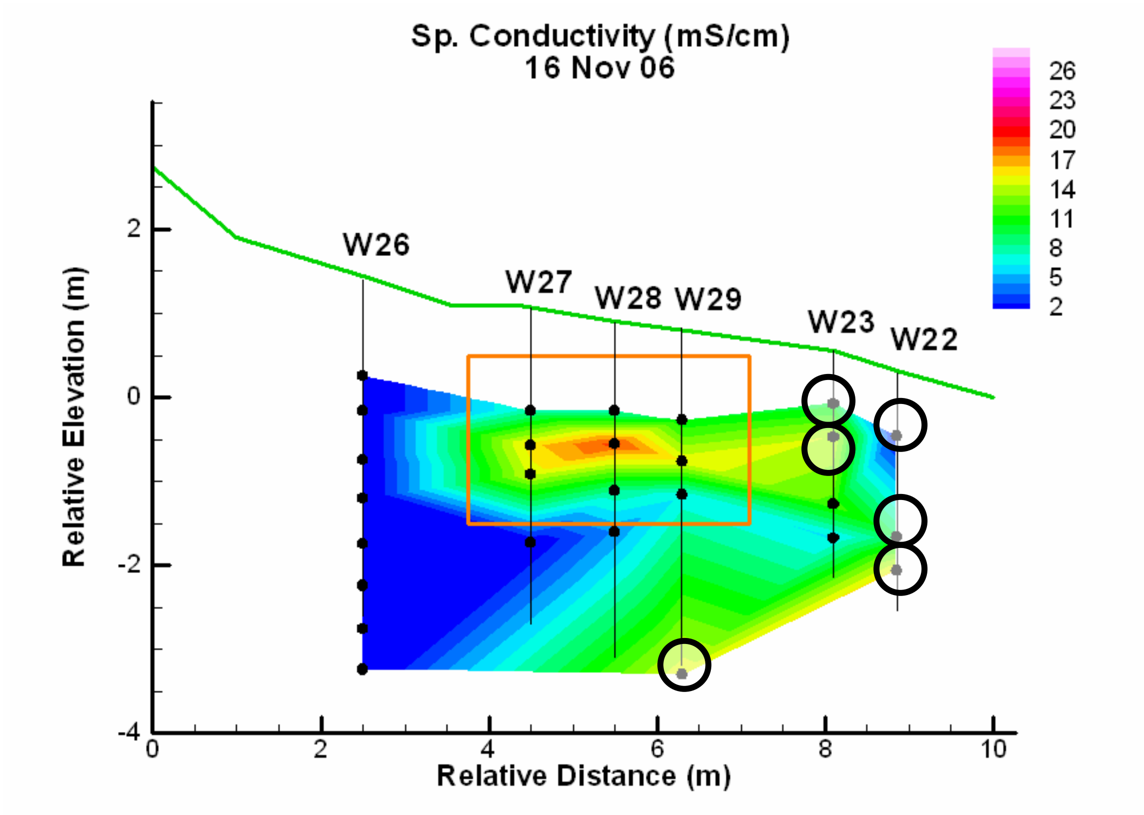
Sp. Conductivity (mS/cm)
16 Nov 06
26
23
20
17
14
11
8
5
2
W26
W27
W28
W29
W23
W22
Relative Elevation (m)
Relative Distance (m)
2
0
-2
-4
0
2
4
6
8
10

Figure 2.

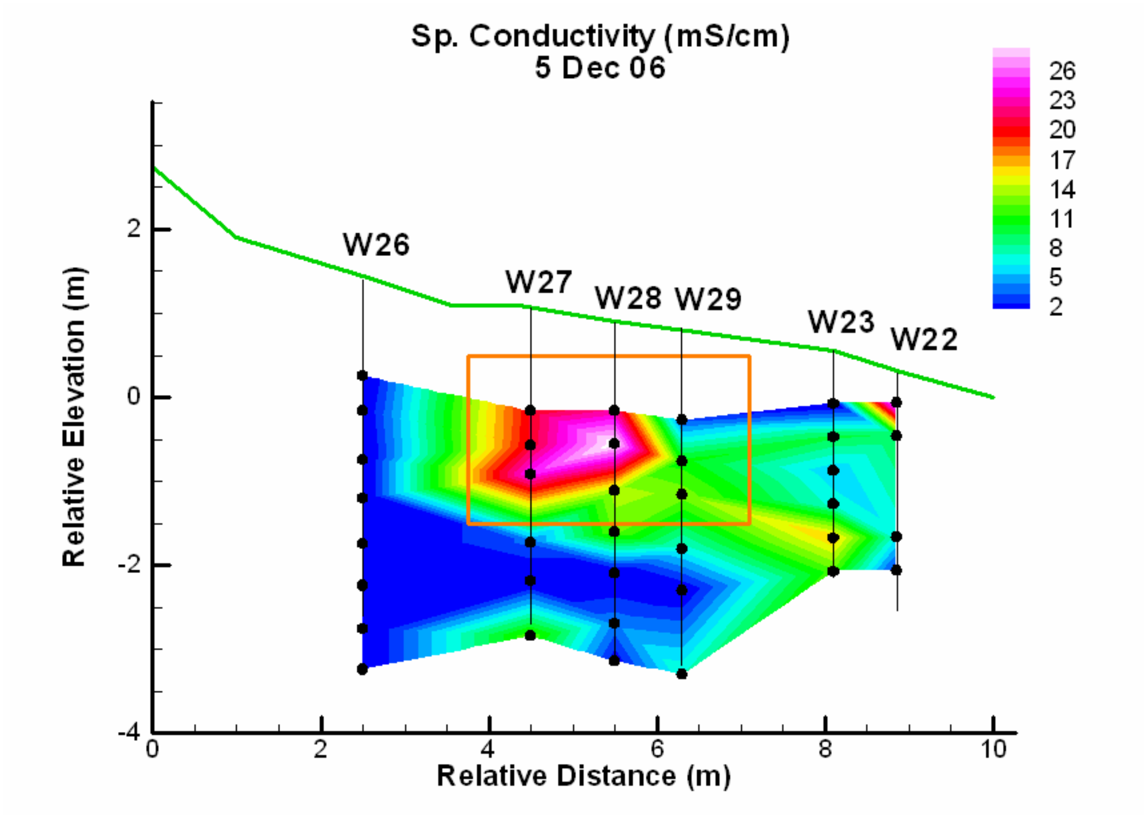
Sp. Conductivity (mS/cm)
5 Dec 06
26
23
20
17
14
11
8
5
2
W26
W27
W28
W29
W23
W22
Relative Elevation (m)
2
0
-2
-4
0
2
4
6
8
10
Relative Distance (m)

Figure 3.

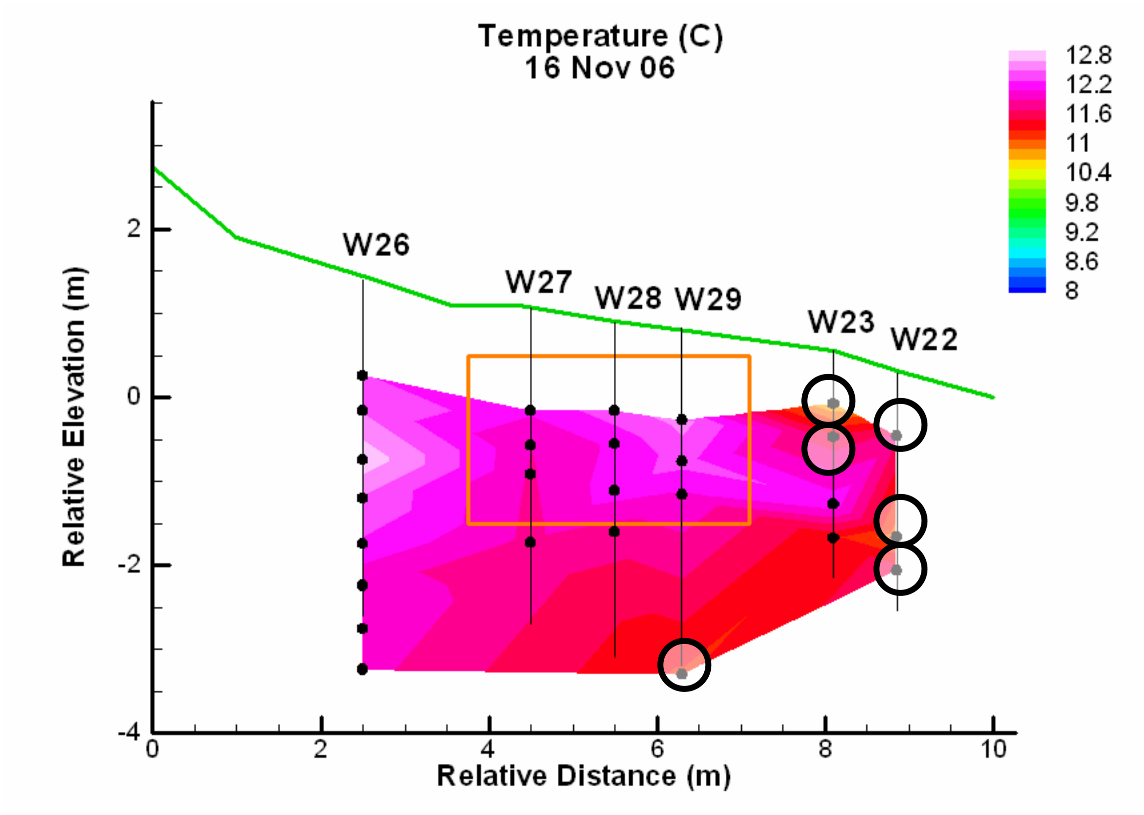

Temperature (C)
16 Nov 06
12.8
12.2
11.6
11
10.4
9.8
9.2
8.6
8
W26
W27
W28
W29
W23
W22
Relative Elevation (m)
Relative Distance (m)
2
0
-2
-4
0
2
4
6
8
10

Figure 4.

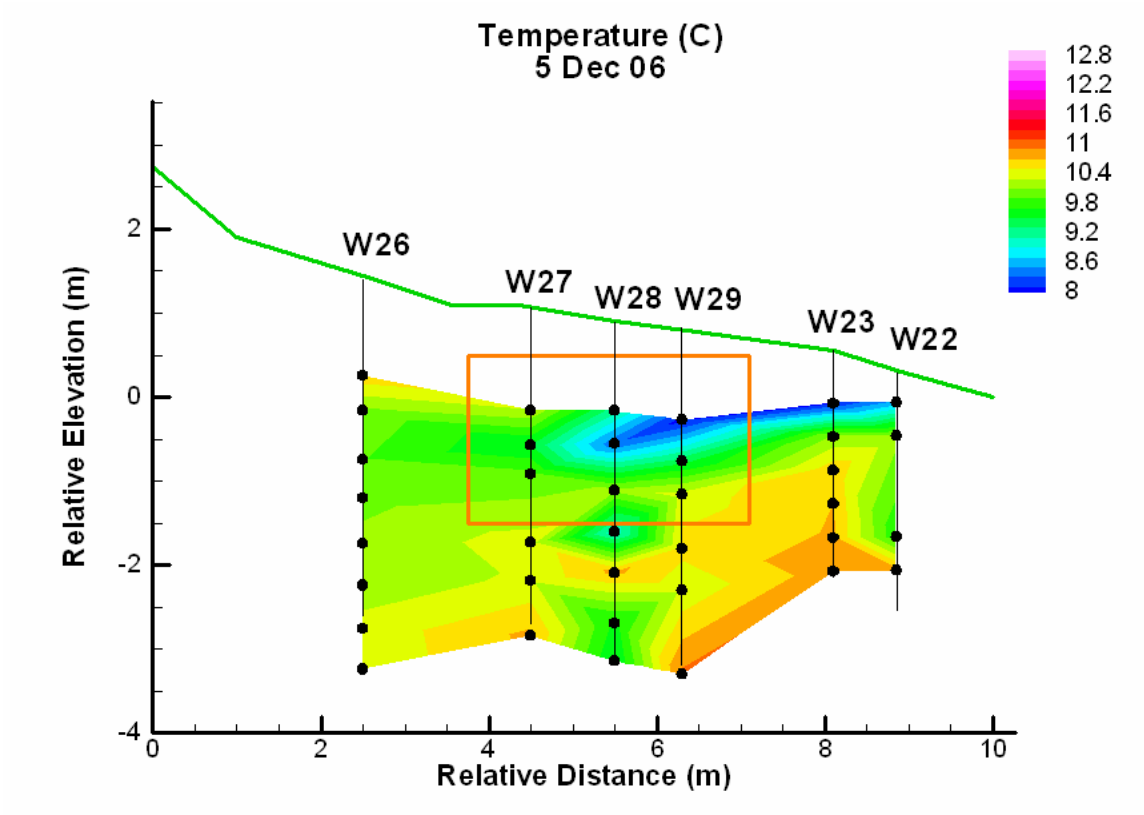

Temperature (C)
5 Dec 06
12.8
12.2
11.6
11
10.4
9.8
9.2
8.6
8
W26
W27
W28
W29
W23
W22
Relative Elevation (m)
2
0
-2
-4
0
2
4
6
8
10
Relative Distance (m)

Figure 5.

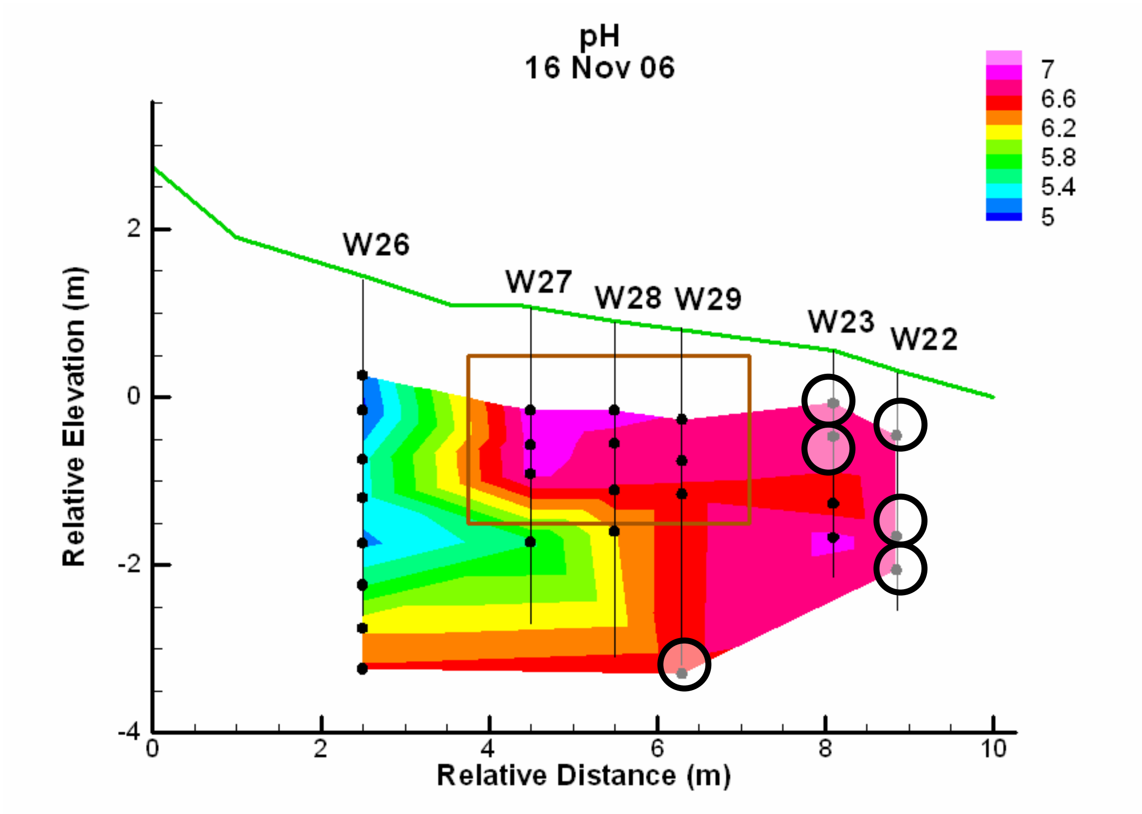
pH
16 Nov 06
7
6.6
6.2
5.8
5.4
5
W26
W27
W28
W29
W23
W22
Relative Elevation (m)
Relative Distance (m)
2
0
-2
-4
0
2
4
6
8
10

Figure 6.

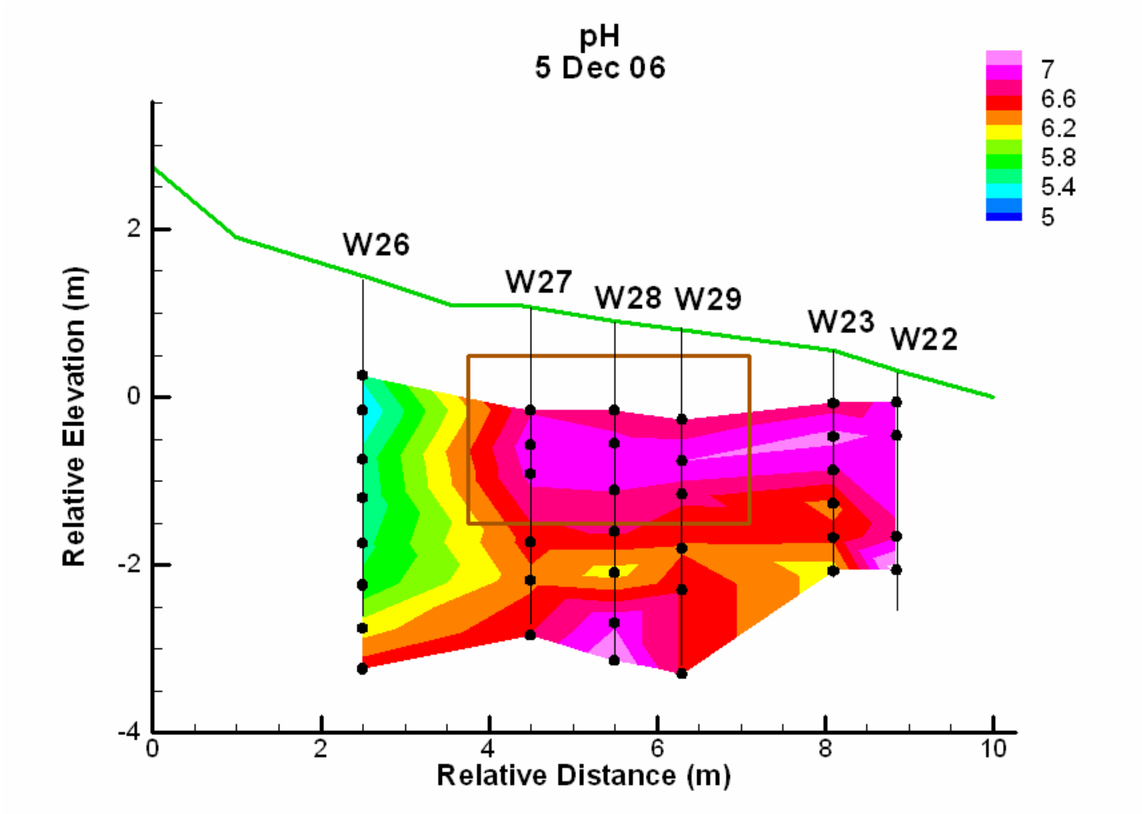

pH
5 Dec 06
7
6.6
6.2
5.8
5.4
5
W26
W27
W28
W29
W23
W22
Relative Elevation (m)
Relative Distance (m)
2
0
-2
-4
0
2
4
6
8
10

Figure 7.

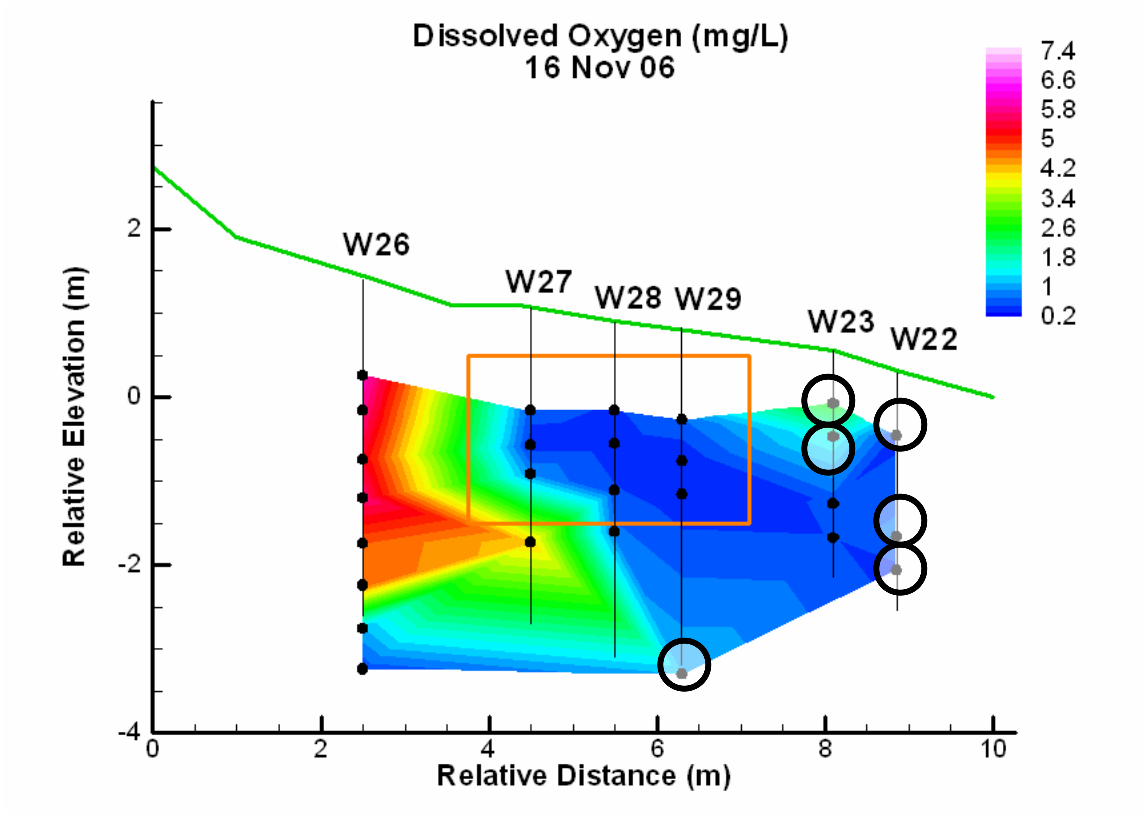
Dissolved Oxygen (mg/L)
16 Nov 06
7.4
6.6
5.8
5
4.2
3.4
2.6
1.8
1
0.2
W26
W27
W28
W29
W23
W22
Relative Elevation (m)
2
0
-2
-4
0
2
4
6
8
10
Relative Distance (m)

Figure 8.

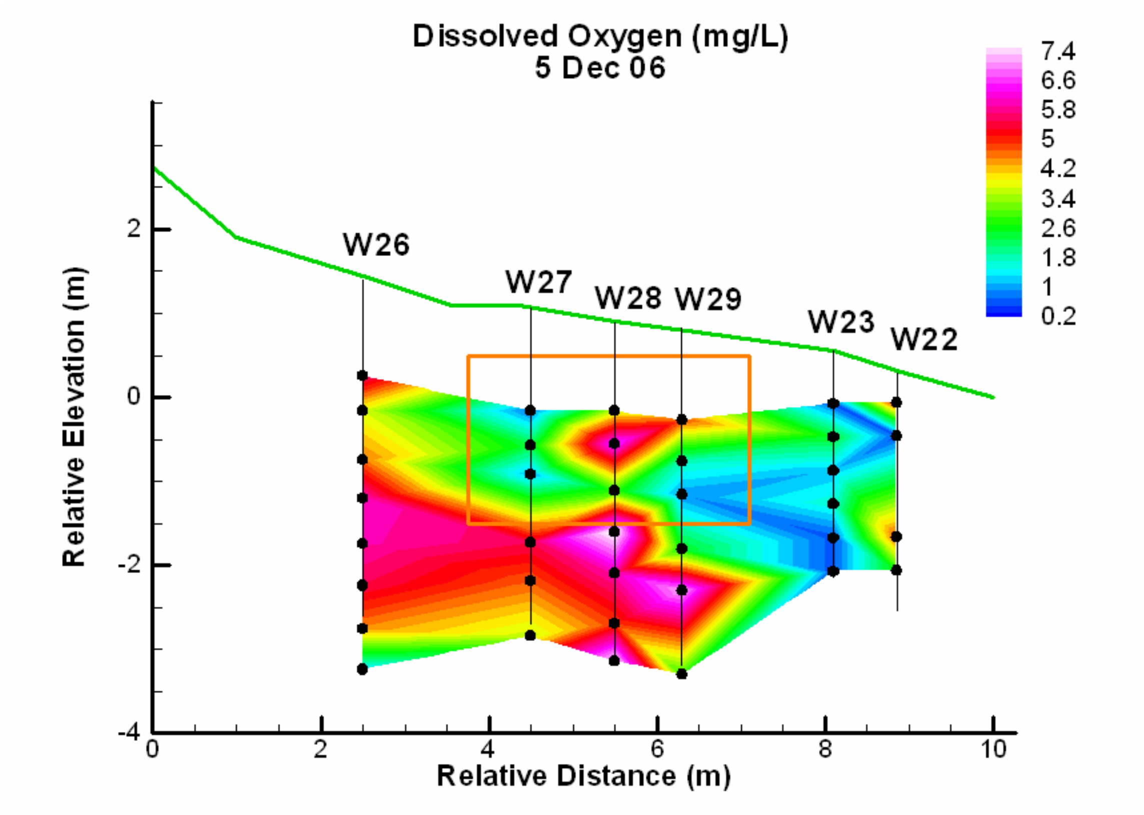
Dissolved Oxygen (mg/L)
5 Dec 06
7.4
6.6
5.8
5
4.2
3.4
2.6
1.8
1
0.2
W26
W27
W28
W29
W23
W22
Relative Elevation (m)
Relative Distance (m)
2
0
-2
-4
0
2
4
6
8
10

Figure 9.

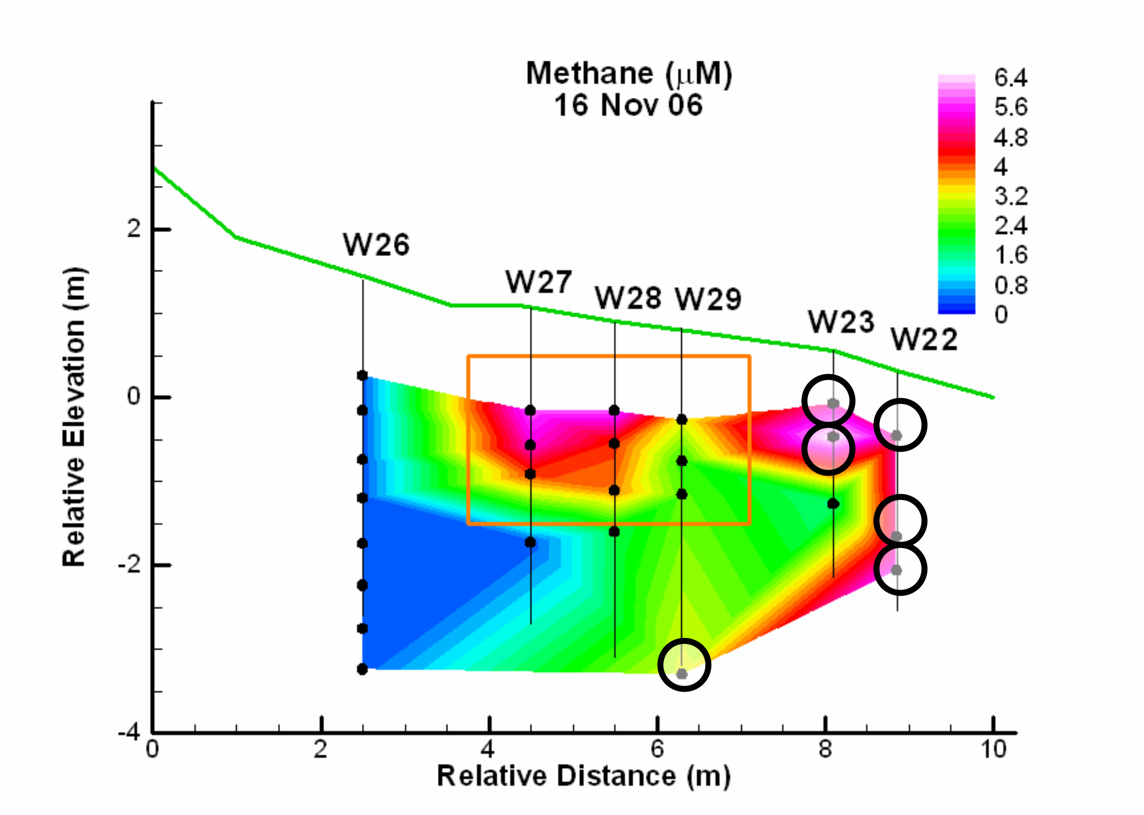
Methane (μM)
16 Nov 06
W26
W27
W28
W29
W23
W22
6.4
5.6
4.8
4
3.2
2.4
1.6
0.8
0
Relative Elevation (m)
2
0
-2
-4
0
2
4
6
8
10
Relative Distance (m)

Figure 10.

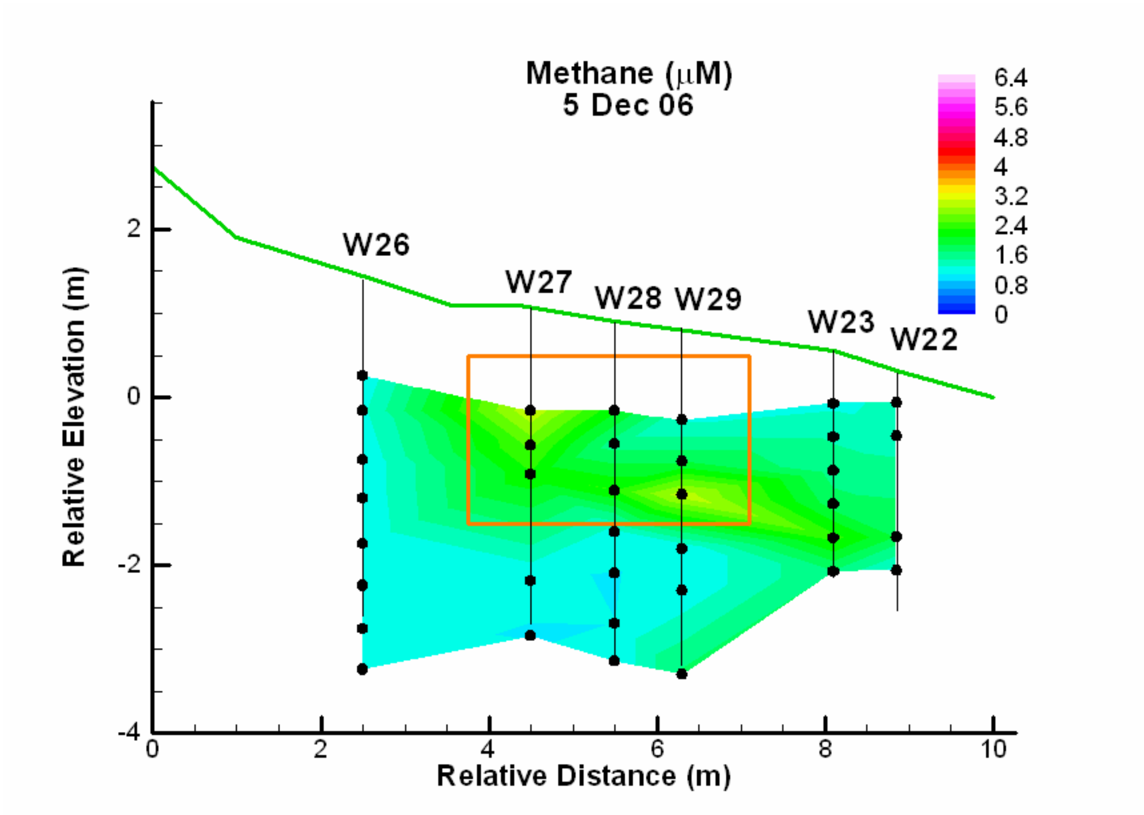

Methane (μM)
5 Dec 06
6.4
5.6
4.8
4
3.2
2.4
1.6
0.8
0
W26
W27
W28
W29
W23
W22
Relative Elevation (m)
Relative Distance (m)
2
0
-2
-4
0
2
4
6
8
10

Figure 11.

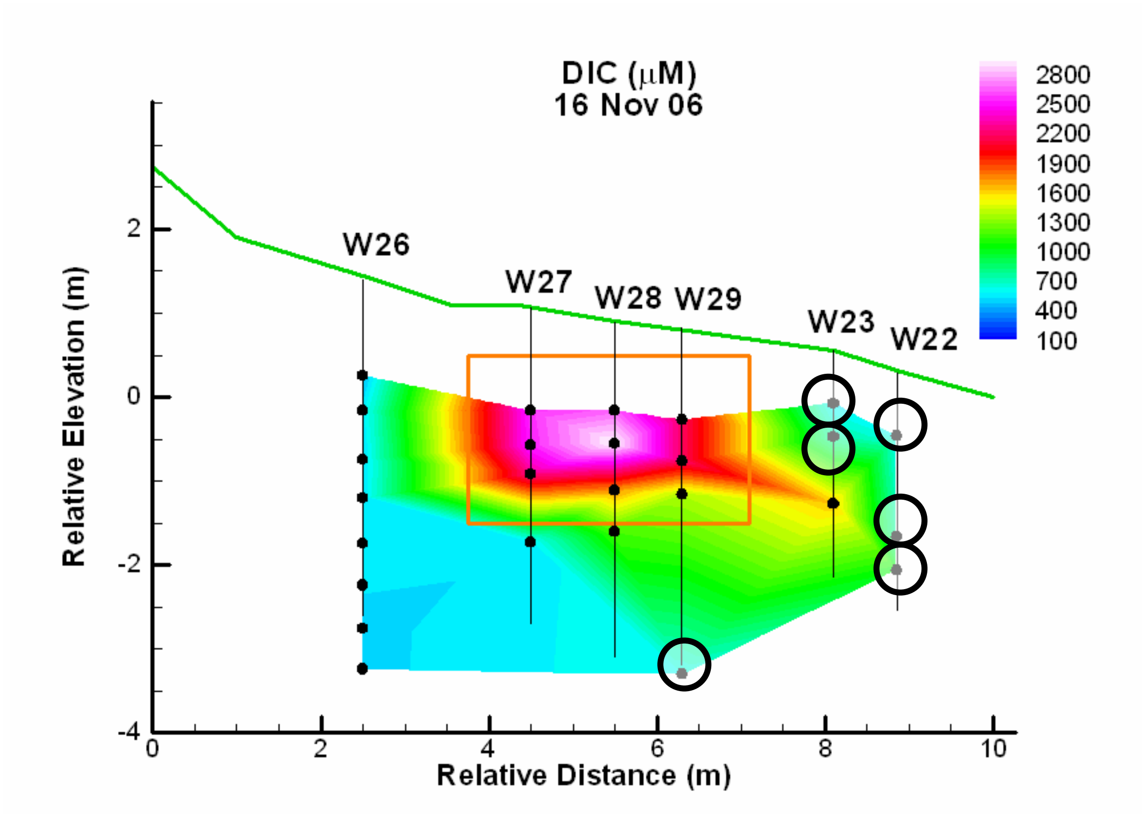
DIC (μM)
16 Nov 06
2800
2500
2200
1900
1600
1300
1000
700
400
100
W26
W27
W28
W29
W23
W22
Relative Elevation (m)
Relative Distance (m)
2
0
-2
-4
0
2
4
6
8
10

Figure 12.

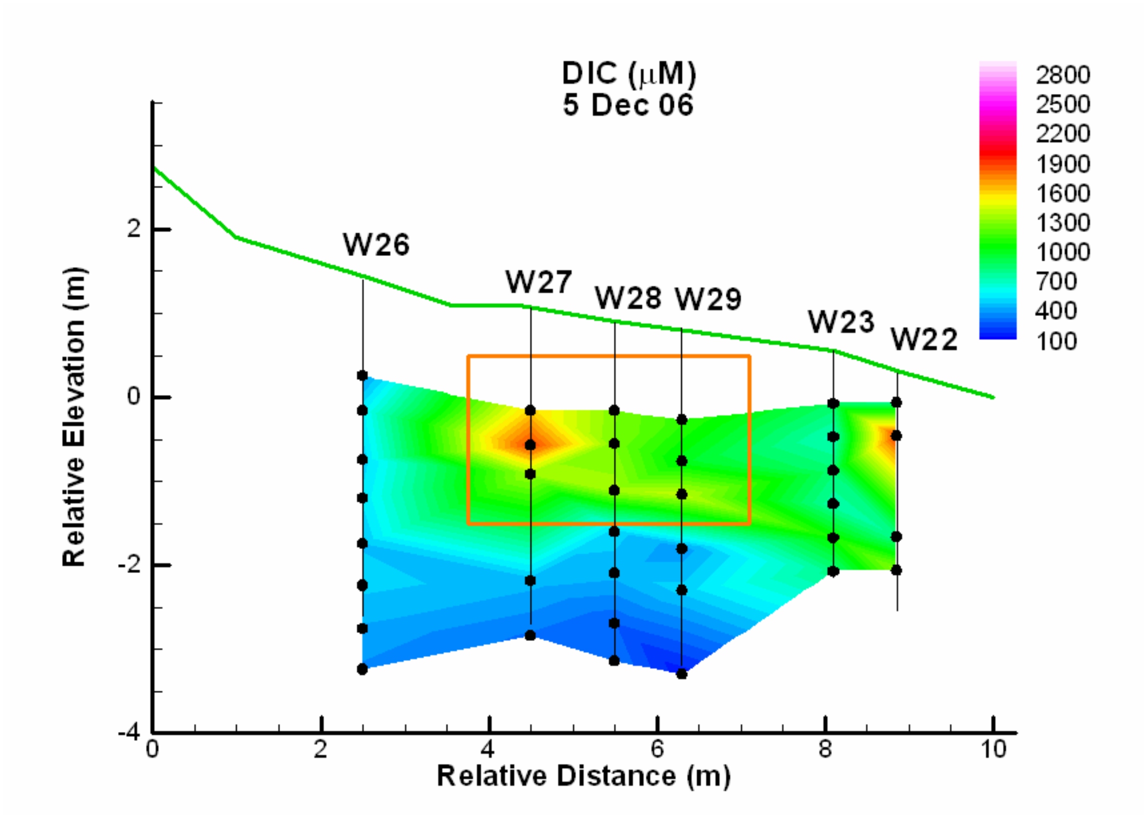
DIC (μM)
5 Dec 06
2800
2500
2200
1900
1600
1300
1000
700
400
100
W26
W27
W28
W29
W23
W22
Relative Elevation (m)
2
0
-2
-4
0
2
4
6
8
10
Relative Distance (m)

Figure 13.